^{31}P NMR Studies of ATP Synthesis and Hydrolysis Kinetics in the Intact Myocardium†

P. B. Kingsley-Hickman,‡ E. Y. Sako,§ P. Mohanakrishnan,‡ P. M. L. Robitaille,‡ A. H. L. From,∥ J. E. Foker,§ and K. Uğurbil*,‡

Department of Biochemistry and Gray Freshwater Biological Institute, University of Minnesota, Navarre, Minnesota 55392, Department of Surgery, University of Minnesota, Minneapolis, Minnesota 55455, and Department of Medicine, Cardiology Division, Minneapolis VA Medical Center and University of Minnesota, Minneapolis, Minnesota 55455

Received April 3, 1987; Revised Manuscript Received June 30, 1987

ABSTRACT: The origin of the nuclear magnetic resonance (NMR)-measurable ATP ⇄ P_i exchange and whether it can be used to determine *net* oxidative ATP synthesis rates in the intact myocardium were examined by detailed measurements of ATP ⇄ P_i exchange rates in both directions as a function of the myocardial oxygen consumption rate (MVO_2) in (1) glucose-perfused, isovolumic rat hearts with normal glycolytic activity and (2) pyruvate-perfused hearts where glycolytic activity was reduced or eliminated either by depletion of their endogenous glycogen or by use of the inhibitor iodoacetate. In glucose-perfused hearts, the P_i → ATP rate measured by the conventional two-site saturation transfer (CST) technique remained constant while MVO_2 was increased approximately 2-fold. When the glycolytic activity was reduced, the P_i → ATP rate decreased significantly, demonstrating the existence of a significant glycolytic contribution. Upon elimination of the glycolytic component, the measured P_i → ATP rates displayed a linear dependence on MVO (micromoles of O consumption rate) with a slope of 2.36 ± 0.15 (N = 8, standard error of the mean). This linear relationship is expected if the rate determined by CST is the *net* rate of ATP synthesis by the oxidative phosphorylation process, in which case the slope must equal the P:O ratio. The ATP → P_i rates and rate:MVO ratios measured by the multiple-site saturation transfer method at two MVO_2 levels were equal to the corresponding P_i → ATP rates and rate:MVO ratios obtained in the absence of a glycolytic contribution. The following conclusions are drawn from these studies: (1) unless the glycolytic contribution to the ATP ⇄ P_i exchange is inhibited or is specifically shown not to exist, the myocardial P_i ⇄ ATP exchange due to oxidative phosphorylation cannot be studied by NMR; (2) at moderate MVO_2 levels, the reaction catalyzed by the two glycolytic enzymes glyceraldehyde-3-phosphate dehydrogenase and 3-phosphoglycerate kinase is near equilibrium; (3) the ATP synthesis by the mitochondrial H^+-ATPase occurs unidirectionally (i.e., the reaction is far out of equilibrium); (4) the "operative" P:O ratio in the intact myocardium under our conditions is significantly less than the canonically accepted value of 3.

In aerobic tissues, ATP synthesis occurs predominantly by the H^+-ATPase of the mitochondria through oxidative phosphorylation. While numerous mechanistic features of this process are well understood, there is a paucity of information about its kinetics in the intact cell. This is primarily due to the extreme difficulty of obtaining such kinetic information by classical biochemical methods. This limitation has been partially overcome with the relatively recent expansion of nuclear magnetic resonance (NMR)[1] spectroscopy to studies of intact cells and tissues. The magnetization transfer techniques of NMR provide the unique capability of studying the kinetics of enzymes in situ [see reviews by Alger and Shulman (1984), Koretsky and Weiner (1984), and Ugurbil (1985a)]. However, even with this methodology, kinetic studies in intact tissues continue to be extremely complex due to the partitioning of enzymatic reactions and their reactants among the various subcellular organelles, and the presence of multiple reactions that utilize the same substrates. Provided that the resonances of the exchanging metabolites are well resolved from each other, the last complication can be eliminated by use of the multiple saturation transfer procedure (Ugurbil, 1985b; Ugurbil et al., 1986). However, analogous solutions to the other complications encountered do not exist. Therefore, prior to reaching any fundamental biochemical conclusions, critical control experiments must be performed to evaluate the validity of the assumptions inherent in the application of magnetization transfer measurements to intact tissues. This is particularly necessary in the study of ATP ⇄ P_i exchange in situ; several different enzymes can contribute to this process in the intact tissue, and, as mediated by oxidative phosphorylation, ATP ⇄ P_i exchange involves transport across the mitochondrial membrane.

† This work was supported by NIH Grants HL33600, HL26640, and 1K04HL01241 and by Veteran's Administration Medical Research funds.

* Address correspondence to this author.

‡ Department of Biochemistry and Gray Freshwater Biological Institute.

§ Department of Surgery.

∥ Department of Medicine.

[1] Abbreviations: AK, adenylate kinase; BCA, 4-bromocrotonic acid; CK, creatine kinase; CP, creatine phosphate; CST, conventional saturation transfer; FBP, fructose 1,6-bisphosphate; FID, free induction decay; GAPDH, glyceraldehyde-3-phosphate dehydrogenase; IA, iodoacetate; LVP, left ventricular pressure; MST, multiple saturation transfer; MVO, myocardial oxygen atom consumption rate in micromoles of O per unit time; MVO_2, myocardial O_2 consumption rate in micromoles of O_2 per unit time; NMR, nuclear magnetic resonance; PGK, 3-phosphoglycerate kinase; 3-PGP, 3-phosphoglyceroyl phosphate (also known as 1,3-diphosphoglycerate); RPP, rate pressure product (the product of heart rate and left ventricular systolic pressure); SD, standard deviation; SEM, standard error of the mean; SP, sugar phosphate; EDTA, ethylenediaminetetraacetic acid; HR, heart rate; EDP, end-diastolic pressure; ATPγ, γ-phosphate of ATP.

0006-2960/87/0426-7501$01.50/0 © 1987 American Chemical Society

Despite the aforementioned difficulties, it is possible to conduct experiments that examine the validity of the saturation transfer studies in the complex environment of the intact cell. In this paper, we describe the results obtained from such detailed measurements of the ATP $\rightleftarrows$ P_i exchange in Langendorff-perfused rat hearts.

Materials and Methods

Perfused Heart Preparation. The perfusion apparatus that allows simultaneous and continuous monitoring of MVO_2, LVP, and NMR spectra and the method of preparation of isovolumic Langendorff-perfused rat hearts have been described in detail previously (Ugurbil et al., 1986). The perfusion medium was a modified, phosphate-free Krebs–Henseleit buffer containing 119 mM NaCl, 5.9 mM KCl, 0.1 mM EDTA, 1.2 mM $MgCl_2$, 28 mM $NaHCO_3$, and 1.8 mM $CaCl_2$. The carbon source was varied for different groups and contained either 11 mM glucose or 0.5–10 mM pyruvate or both. The specific carbon substrate conditions are given for each experiment described under Results. When sodium pyruvate was used, NaCl concentration was decreased by the same amount. The left ventricle was vented as before (Ugurbil et al., 1986). The perfusion pressure was 107 mmHg. The average coronary flow in hearts not exposed to dobutamine or IA was 21 ± 6 (SD) mL/min. The coronary flow increased when dobutamine was added.

Cardiac Performance. The different levels of MVO_2 and mechanical output were achieved by using four different states of the heart rate (HR), end-diastolic pressure (EDP), and exposure to the inotrope dobutamine. These states were the following: (i) HR = 300/min, EDP = 4–8 mmHg, no dobutamine; (ii) HR = 420/min, EDP = 4–8 mmHg, 50 ng/mL dobutamine in the perfusate; (iii) HR = 480/min, EDP = 16–20 mmHg, 80 ng/mL dobutamine; (iv) HR = 600/min, EDP = 24 mmHg, 80 ng/mL dobutamine. In hearts where GAPDH was inhibited by IA, a fifth work state (which we will call i′) characterized by HR = 366, EDP = 8–12 mmHg, and 20 ng/mL dobutamine was employed. This work state generated MVO_2 values in between those achieved during work states i and ii. It should be noted that the carbon substrate conditions were also altered in addition to altering the work states. This influenced the MVO_2 and RPP achieved by the hearts at the various work states.

IA Inhibition of GAPDH. Subsequent to experiments conducted to evaluate the minimum dose of IA required for GAPDH inhibition, the protocol chosen was infusion of IA through a side port in the inflow line to achieve 0.15 mM IA in the perfusate for 15 min and subsequent reduction of the IA concentration in the perfusate to 0.025 mM. The low IA concentration was maintained throughout the kinetic measurements.

The kinetic studies with IA-inhibited hearts were conducted at work states i, i′, ii, and iv. These hearts were supplied with 0.5, 0.5, 1, and 10 mM pyruvate at work states i, i′, ii, and iv, respectively.

Depletion of Endogenous Carbon Sources. Transient perfusion with substrate-free medium was employed to reduce endogenous glycogen and, thus, the endogenous carbon substrate available to GAPDH. With substrate-free medium, the hearts maintained a constant LVP for approximately 15–25 min; subsequently, the LVP declined unless a carbon source was supplied. On the hearts prepared for the kinetic studies, the carbon substrate infusion was commenced when the LVP declined to between 75% and 50% of the initial steady-state value. As discussed further on, this procedure did not induce any functional impairment or nucleotide loss.

NMR Measurements. ^{31}P NMR measurements were recorded on a Nicolet WB360 spectrometer at 146.1 MHz with a single-turn solenoidal probe and balance-tuned circuitry of our design and manufacture. ATP synthesis rates were measured by CST,[2] saturating the ATPγ resonance and observing the P_i resonance. To determine the rate of ATP synthesis, 8 or 10 spectra were recorded by using 90° pulses and a list of different repetition times. FID's were acquired by cycling through this list 24 times, summing 12 FID's each time. One of the 8 or 10 spectra was obtained with a 5–6-s repetition time (allowing full relaxation of the P_i resonance), with the saturating radiation positioned 1100 Hz downfield from P_i, a distance equal to the frequency separation between P_i and ATPγ. The remaining spectra were acquired while saturating ATPγ, with repetition times ranging from 0.3 to 3.5 s; the exact times were varied to assure accurate measurement of the T_1 and the fractional decrease in P_i intensity. These spectra constitute a progressive saturation sequence executed while ATPγ magnetization is nulled; the P_i intensities obtained from this sequence were fitted to the equation $M(\tau) = M'[1 - \exp(-\tau/T_1^*)]$ where M' and T_1^* are the P_i intensity and the spin–lattice relaxation time, respectively, when ATPγ magnetization was saturated and τ is the interpulse delay. Two parameters, M' and T_1^*, were determined by the nonlinear least-squares fit to the data. From M' and the spectra recorded in the absence of ATPγ saturation, the fractional reduction ($\Delta M/M^0$) undergone by the P_i resonance upon irradiation of the ATPγ spins was calculated. $\Delta M/M^0$ is defined as $(M^0 - M')/M^0$ where M^0 is the thermal equilibrium magnetization of the P_i spins and corresponds to the fully relaxed P_i intensity in the absence of any selective irradiation of ^{31}P spins. The pseudo-first-order rate constant k_1 was calculated from the T_1^* and $\Delta M/M^0$ values by the equation $k_1 = (\Delta M/M^0)/T_1^*$. The $P_i \rightarrow$ ATP rate, or flux, is simply $k_1[P_i]$. The saturating frequency was on at all times except during acquisition of the FID's, which took 64 ms. In addition, for each heart, a fully relaxed spectrum (15-s repetition time) was recorded with no saturating radiation, both before and after the kinetic measurements. These spectra were used to calculate the ATP, CP, and P_i content of the hearts using integrated intensities and the resonance from the 100 mM phenylphosphonate solution contained in the latex balloon inserted in the left ventricle.

Except for the specific resonances saturated, the number of FID's accumulated, and the pulse repetition times employed, the MST procedure employed to measure ATP hydrolysis rates was identical with that described previously (Ugurbil et al., 1986). For the experiments reported here, 11 spectra were recorded, 2 of them with a 2.5-s repetition time, with the f2 frequency set 1100 Hz upfield from ATPγ, and 9 of them with 8 different repetition times varying from 0.2 to 2.5 s while the P_i resonance was saturated. CP was saturated by using selective irradiation f1 during all 11 spectra. Spectra to determine sigma (σ) (Ugurbil, 1985b) were collected both before and after the kinetic measurements.

Results

$P_i \rightarrow$ ATP Rate in Glucose-Perfused Hearts. Glucose is a major carbon source for the cardiac muscle and is commonly used in perfused heart studies. Therefore, we undertook CST measurements of the $P_i \rightarrow$ ATP rate at four different levels of RPP and MVO_2 in glucose-perfused hearts. Typical spectra obtained during the kinetic measurements at the lowest and highest MVO_2's attained (work states i and iv, respectively)

[2] We will refer to the two-site saturation transfer measurements as CST.

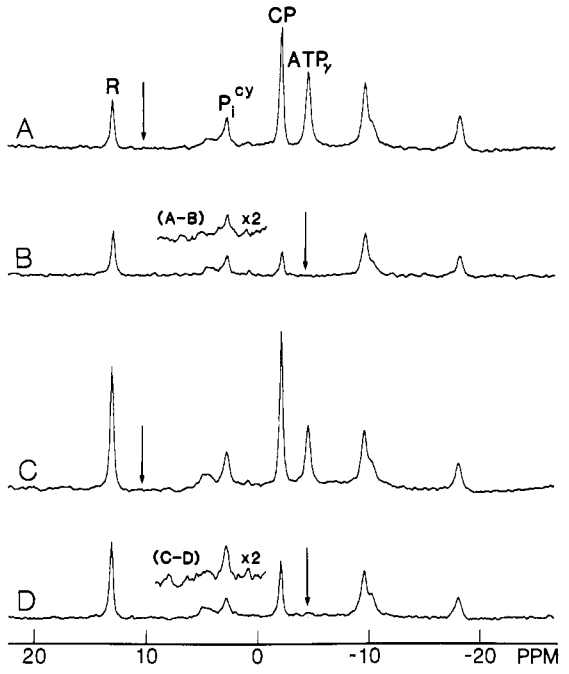

FIGURE 1: ^{31}P NMR spectra showing saturation transfer at work states i (A and B) and iv (C and D). The position of the selective irradiating frequency is indicated by the arrows. R is a 100 mM phenylphosphonate reference in an intraventricular balloon; P_i^{cy}, cytosolic inorganic phosphate; CP, creatine phosphate; ATPγ, γ-phosphate of ATP. For each spectrum, 288 FID's were accumulated with 90° pulses, 64-ms acquisition time, and an interpulse delay of 5 s (A and C) or 2.8 s (B and D). Because the T_1 of P_i decreases when ATPγ is saturated, the P_i resonance is fully relaxed in each spectrum. Other resonances such as R and CP are not fully relaxed. The difference spectra in the P_i region are shown as insets with the vertical scale expanded 2-fold for clarity. Both hearts were perfused with 11 mM glucose; in addition, the heart in work state iv had 3 mM pyruvate, resulting in a higher CP concentration and CP:ATP ratio.

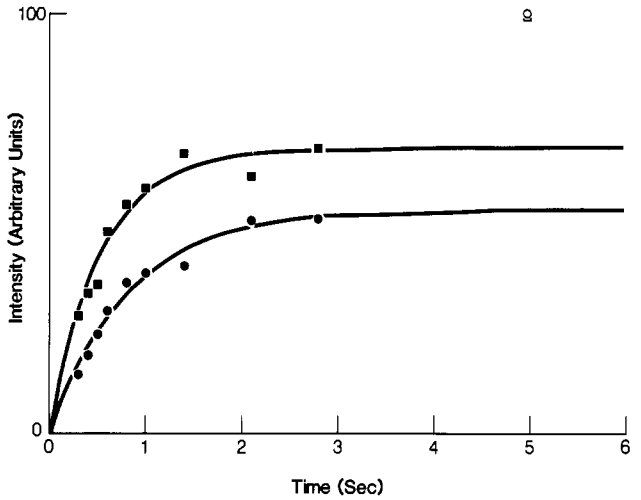

FIGURE 2: Measurement of T_1 and $\Delta M/M^0$ for P_i during saturation transfer in representative hearts at two different work states (i and iv). The selective radio-frequency irradiation was on the ATPγ resonance for the closed symbols (■ and ●) and in the control position for open symbols (□ and ○). (□ and ■) Work state i; (○ and ●) work state iv. For each point, 288 FID's were acquired in a time-averaged manner as described in the text and Figure 1 legend.

are illustrated in Figure 1. The two spectra shown for each work state were taken from a series of spectra recorded in a time-averaged fashion for the determination of the $P_i \rightarrow$ ATP rate as described under Materials and Methods. The P_i intensities from complete sets of measurements performed at work states i and iv are illustrated in Figure 2; the solid lines in this figure are the best fits obtained by the two-parameter

Table I: Unidirectional $P_i \rightarrow$ ATP Rate in Glucose-Perfused Hearts at Four Different Work States That Achieved Different Oxygen Consumption Rates[a]

	i (N = 10)	ii (N = 10)	iii (N = 10)	iv (N = 12)
$P_i \rightarrow$ ATP rate [μmol s^{-1} (g·dry wt)$^{-1}$]	7.1 ± 0.8	7.3 ± 0.5	7.5 ± 0.7	6.5 ± 0.9
rate:MVO ratio	6.4 ± 0.8	4.5 ± 0.2	4.0 ± 0.3	2.9 ± 0.3
T_1* (s)	0.59 ± 0.03	0.78 ± 0.03	0.78 ± 0.03	1.03 ± 0.07
$\Delta M/M^0$	0.34 ± 0.03	0.32 ± 0.01	0.49 ± 0.01	0.44 ± 0.02
k_1 (s)[b]	0.61 ± 0.08	0.43 ± 0.03	0.64 ± 0.04	0.46 ± 0.05

[a] All values are mean ± SEM. N is the number of hearts on which these measurements were performed. The specific conditions for work states i–iv are given under Materials and Methods. MVO is the rate of oxygen *atom* consumpation by the heart. $\Delta M/M^0$ is the fractional reduction in P_i intensity induced by saturating the ATPγ spins. T_1* is the P_i spin–lattice relaxation rate when ATPγ spins are nulled. [b] k_1 is the pseudo-first-order rate constant for the $P_i \rightarrow$ ATP reaction.

Table II: Metabolic and Functional Properties Displayed by Glucose-Perfused Hearts during $P_i \rightarrow$ ATP Rate Measurements at Four Different Work States[a]

	i (N = 10)	ii (N = 10)	iii (N = 10)	iv (N = 12)
ATP content [μmol (g·dry wt)$^{-1}$]	23.5 ± 2.0	21.2 ± 0.8	18.1 ± 1.6	18.8 ± 1.2
P_i content [μmol (g·dry wt)$^{-1}$]	11.9 ± 0.7	17.2 ± 0.7	11.6 ± 0.9	14.0 ± 1.1
RPP (10^3 mmHg min^{-1})	26.4 ± 2.0	57.1 ± 2.6	71.3 ± 1.9	81.2 ± 2.0
MVO_2 [μmol min^{-1} (g·dry wt)$^{-1}$]	34.0 ± 2.2	48.8 ± 3.1	56.7 ± 1.9	66.6 ± 2.5

[a] All values are mean ± SEM. In work states iii and iv, the perfusate was supplemented with 2 and 3 mM pyruvate, respectively.

fit of the data points recorded while saturating ATPγ. The kinetic and metabolic data for all work states examined are summarized in Tables I and II. The MVO_2, RPP, and levels of ATP and P_i given in Table II correspond to the average values maintained by hearts during the saturation transfer experiments. Despite the relatively long time of data acquisition (~80 min), the MVO_2 and RPP achieved and maintained at the different work states were linearly dependent as they should be (Kobayashi & Neely, 1979).

The T_1* and $\Delta M/M^0$ for the P_i resonance increased with increasing MVO_2 while neither the $P_i \rightarrow$ ATP rate nor the P_i concentration displayed commensurate variations, indicating that the T_1 of P_i spins in the *absence* of the ATP $\rightleftarrows$ P_i exchange varied with work load; this T_1 is equal to T_1*/(1 − $\Delta M/M^0$) and is calculated to be 0.90 ± 0.04, 1.14 ± 0.03, 1.54 ± 0.05, and 1.82 ± 0.07 s (all errors are SEM) for work states i–iv, respectively.

Glucose-perfused hearts cannot maintain a steady-state MVO_2 and mechanical output for prolonged periods of time at high work loads. Therefore, for the work states iii and iv, the perfusate was supplemented with 2 and 3 mM pyruvate, respectively; these pyruvate levels are not sufficient to maximally activate pyruvate dehydrogenase (Dennis et al., 1979) or fully inhibit glycolysis. Consequently, the metabolism continues to rely heavily on glucose consumption. The inclusion of pyruvate is responsible for the fact that P_i levels attained at the higher cardiac performance of work states iii and iv (Table II) remained comparable to the P_i level displayed at work state i. On glucose alone, the P_i content would have been significantly greater (From et al., 1986).

The data presented in Tables I and II were obtained by calculating all the parameters of interest for each heart and

Table III: Kinetic Data on $P_i \rightarrow ATP$ Rate Obtained on Glucose-Perfused Hearts at Two Work States Analyzed by a Different Method[a]

	ii	iii
$\Delta M/M^0$	0.32 ± 0.01	0.49 ± 0.02
T_1* (s)	0.81 ± 0.01	0.82 ± 0.02
k_1 (s^{-1})	0.40 ± 0.01	0.60 ± 0.03

[a] In this method, the spectra from all 10 hearts at each work load were summed. $\Delta M/M^0$ and T_1* were obtained from this global sum. Errors for T_1* were obtained from the fit to data. Errors for the $P_i \rightarrow$ ATP rate were calculated from errors in $\Delta M/M^0$, T_1*, and P_i content.

subsequently analyzing them to obtain the mean, the SD, and SEM. The raw data were also analyzed by a second method where the corresponding spectra recorded from the different hearts at a given work state were summed and the necessary kinetic parameters were calculated directly from this resultant set of spectra. Table III gives the results obtained with the second method for two of the work states. Comparison with the corresponding data in Table I clearly demonstrates that the values generated from our data by the two different methods of analysis are essentially the same. The two methods can yield significantly different results only if the observed differences among hearts are dominated by a relatively poor signal-to-noise level of each determination rather than by actual variations among the different hearts, and if the number of measurements performed is not sufficiently large.

Glycolytic Contribution to the $P_i \rightarrow ATP$ Rate. It is possible that the glycolytic enzymes GAPDH and PGK together can catalyze $P_i \rightleftarrows$ ATP exchange through the phosphorylated intermediate 3-PGP and contribute to the NMR-measured $P_i \rightarrow$ ATP rate. The existence of such a glycolytic contribution was recently demonstrated in yeast (Brindle & Krikler, 1985; Campbell et al., 1985) and liver (Thoma & Ugurbil, 1987).

In order to evaluate experimentally the origin of the saturation transfer effect in the myocardium, $P_i \rightarrow$ ATP rate measurements were repeated in hearts where the overall glycolysis rate, specifically the GAPDH/PGK activity, was reduced or eliminated. This reduction was achieved by using the following three different approaches: (1) Glucose was replaced with a small but sufficient amount of pyruvate to reduce the carbon substrate flow into the glycolytic pathway. (2) In addition to the use of pyruvate as the exogenous substrate, endogenous carbon sources for glycolysis were depleted as described under Materials and Methods. (3) GAPDH was inhibited with low concentrations of IA.

In all cases, the amount of pyruvate supplied was dependent on the work load and was kept low (except at the work state with the highest RPP and MVO_2) in order to achieve P_i levels that were comparable to those attained at low work loads when glucose was the primary carbon source, and to prevent the diversion of excess pyruvate to the synthesis of GAPDH/PGK substrates through gluconeogenesis.

The GAPDH/PGK contribution to the $P_i \rightarrow$ ATP rate can, in principle, be eliminated by using MST, thereby avoiding the use of IA or substrate manipulations. This, however, requires selective irradiation of the acyl phosphate resonance of 3-PGP. This resonance is not visible in the intact heart spectra. Irradiating in the −5 to 0 ppm region [which covers the chemical shift range previously reported for the 3-PGP acyl phosphate (Nageswara Rao et al., 1978, 1979)] displayed no detectable effect on the P_i resonance. This implies either that due to a very short lifetime, the acyl phosphate of 3-PGP requires very high power to saturate or else that its chemical shift in the tissue is outside of the range searched. Therefore, substrate manipulation and IA inhibition were the only methods used to eliminate the GAPDH/PGK activity in the experiments reported here.

Evaluation of IA Effect on Cardiac Function and Metabolism. Prior to conducting any kinetic measurements, the effects of IA on the nucleotide pools, the cardiac performance, and the myocardial GAPDH activity were evaluated in trial experiments. The left ventricular pressure tracings from glucose- and pyruvate-perfused hearts exposed to IA levels employed in the kinetic studies are illustrated in Figure 3. In order to eliminate the complication arising from endogenous fatty acid utilization, fatty acid metabolism was blocked by BCA in the trial experiments shown in Figure 3A,B,E. BCA was not used during the kinetic measurements and for the heart whose LVP trace is shown in Figure 3C,D. We and others have previously shown that BCA at low doses selectively inhibits fatty acid utilization without adversely influencing the glycolytic or oxidative metabolism directly (Hutter et al., 1984; From et al., 1986).

In hearts perfused initially with 11 mM glucose as the only carbon source, the developed pressure began to decline within ~5 min of IA exposure (Figure 3A). ^{31}P NMR spectra recorded concurrently displayed an extremely large reduction in the CP and ATP content while a large SP peak, attributable predominantly to FBP, appeared (Figure 4A,B). If glucose infusion was continued, the contractile activity ceased completely (Figure 3A).

In a second glucose-perfused heart after all the mechanical activity had ceased following IA exposure, glucose was replaced with pyruvate as the exogenous carbon source (Figure 3B). Pyruvate metabolism does not require the GAPDH activity. With pyruvate infusion, contractile activity resumed and gradually increased toward a new steady state (Figure 3B). The ^{31}P NMR spectrum recorded from this heart in this steady state (Figure 4C) shows that the P_i level was high and ATP level was low. This is due to the loss of nucleotide precursors during the period immediately preceding the infusion of pyruvate, when carbon substrates were not available for ATP synthesis.

Figure 3C illustrates a left ventricular pressure trace obtained from a heart that was perfused with pyruvate from the beginning; glucose was not included in the perfusate, and fatty acid metabolism was not blocked by BCA. This situation is identical with that used in the kinetic measurements. Under this substrate condition, exposure to IA did not induce a precipitous decline in the developed pressure (Figure 3C) nor was there a noticeable accumulation of SP or a reduction in ATP levels (Figure 5A,B). Figure 3D illustrates the pressure tracing from the same heart at a much later time, when pyruvate was replaced by glucose. This substrate switch elicited a dramatic reduction in contractile activity and a rise in the diastolic pressure; concurrently, the heart accumulated high levels of SP (predominantly FBP) and lost its ATP and CP (Figure 5D). The small amount of pressure the heart continued to develop subsequent to switching the carbon substrate to glucose was entirely due to fatty acid utilization. This was shown in a different heart that had been treated identically except that the fatty acid metabolism was blocked with BCA (Figure 3E). When this heart had functioned for approximately 45 min following IA inhibition of GAPDH, the carbon source was switched from pyruvate to glucose; it is seen that in this case the effect on mechanical activity was complete (Figure 3E).

The extent of the GAPDH inhibition by the IA exposure protocol used was evaluated more quantitatively in an IA-inhibited heart that had been depleted of its endogenous gly-

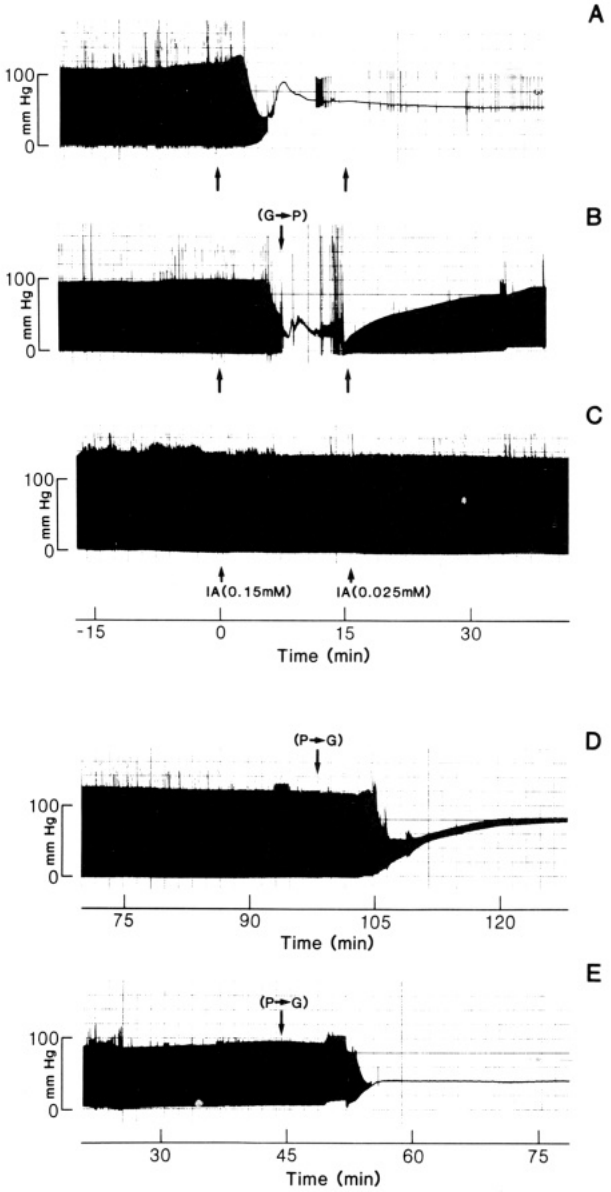

FIGURE 3: Tracings of left ventricular pressure, showing the effects of iodoacetate (IA) on hearts perfused with either 11 mM glucose (G) or 1 mM pyruvate (P) as the carbon source. Glucose, pyruvate, and IA were added through side ports so that their concentrations could be changed quickly. There was a delay of about 1 min before any change reached the heart. Hearts for (A) and (B) were in work state i; hearts for (C), (D), and (E) were in work state ii. ^{31}P NMR spectra from these hearts are shown in Figures 5 and 6. BCA was added to the perfusate for the hearts in (A), (B), and (E). (A) Glucose-perfused heart. IA (0.15 mM) was added at the first arrow and decreased to 0.025 mM at the second arrow. (B) As in (A), but the carbon source was switched from glucose to pyruvate at the time indicated. (C) Pyruvate-perfused heart. (D) The same heart as in (C) at a later time. The carbon source was switched from pyruvate to glucose at the time indicated. (E) Pyruvate-perfused heart, inhibited with IA beginning at 0 min; the carbon source was switched from pyruvate to glucose at the time indicated; this heart was treated similar to that shown in (C) and (D) except BCA was added to the perfusate to inhibit fatty acid metabolism.

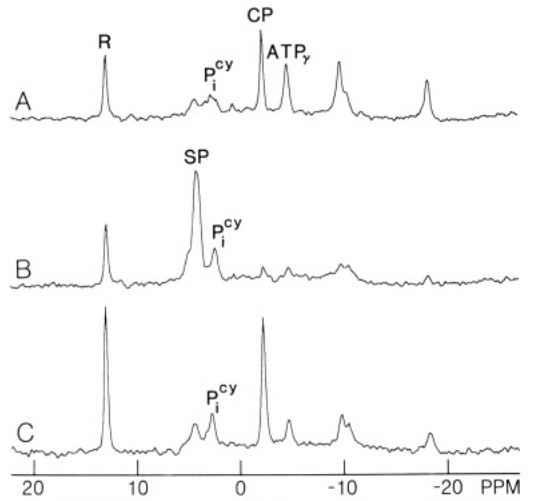

FIGURE 4: ^{31}P NMR spectra of the hearts in Figure 3A,B. SP, sugar phosphates (phosphomonoesters); other peaks are labeled as in Figure 1. For each spectrum, 64 FID's were summed with a 10-s interpulse delay and processed with 30-Hz line broadening. (A) Spectrum recorded immediately prior to IA infusion (see Figure 3A). (B) Spectrum from the same heart as in (A) but 5–15 min after IA infusion (see Figure 3A). The SP peak is mostly fructose 1,6-bisphosphate. (C) Spectrum from a different heart at 40–50 min after IA infusion, when glucose was replaced by pyruvate (see Figure 3B).

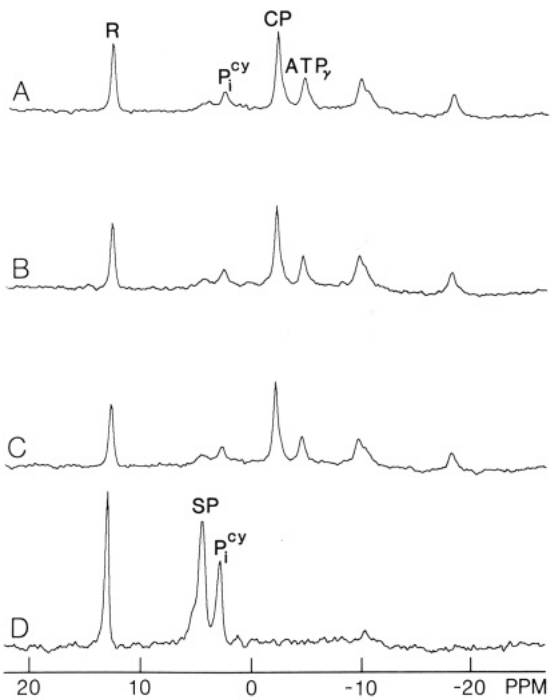

FIGURE 5: ^{31}P NMR spectra of the hearts in Figures 3C–E. Spectral parameters and labeling of resonances are the same as in Figure 4. (A) Immediately prior to IA infusion (see Figure 3C). (B) 15–25 min after IA infusion (see Figure 3C). (C) Immediately prior to switching from pyruvate to glucose (see Figure 3D). (D) 30–40 min after switching from pyruvate to glucose (see Figure 3E).

cogen. In this heart, the replacement of pyruvate with glucose as the carbon source for 1 min led to the appearance of a prominent SP resonance in the ^{31}P NMR spectrum. When the glucose infusion was discontinued and pyruvate infusion resumed, this SP peak disappeared at the rate of 0.008 μmol s^{-1} (g·dry wt)$^{-1}$. This is approximately 10^3 times slower than the maximum $P_i \rightarrow$ ATP flux measured in glucose-perfused hearts. Since the endogenous carbohydrate pool was depleted and perfusion with glucose was very brief, the disappearance of the SP resonance should reflect the sum of GAPDH and fructose 1,6-bisphosphatase activity. Consequently, it is reasonable to conclude that at this level of inhibition, GAPDH/PGK-catalyzed ATP $\rightleftarrows$ P_i exchange cannot possibly contribute to the $P_i \rightarrow$ ATP rate measured by NMR.

$P_i \rightarrow$ ATP Rate in the Absence of GAPDH/PGK Activity. Figure 6 illustrates the MVO_2 vs RPP relationship for all the work states examined in hearts where GAPDH activity was inhibited either by IA or by eliminating exogenous and/or

Table IV: Comparison of MVO_2, RPP, and Kinetic Data Obtained during $P_i \rightarrow ATP$ Rate Measurements in Glucose-Perfused, Pyruvate-Perfused, Pyruvate-Perfused Subsequent to Depletion of Endogenous Carbohydrates, and IA-Inhibited Hearts at Two Work States[a]

	T_1* (s)	$P_i \rightarrow ATP$ rate [μmol s^{-1} (g·dry wt)$^{-1}$]	MVO_2 [μmol min^{-1} (g·dry wt)$^{-1}$]	$P_i \rightarrow ATP$ rate:MVO ratio	RPP (10^3 mmHg min^{-1})
work state i					
control (N = 10)[a] (glucose perfused)	0.59 ± 0.03	7.1 ± 0.8	34.0 ± 2.2	6.4 ± 0.8	26.4 ± 2.0
Pyr perfused (N = 9)[b] (no glucose, depleted)[b]	0.84 ± 0.08	5.0 ± 0.9	36.1 ± 1.5	4.3 ± 0.9	26.5 ± 1.0
Pyr perfused, IA inhibited (N = 9)	0.73 ± 0.05	3.1 ± 0.4	39.5 ± 1.5	2.2 ± 0.3	22.1 ± 1.4
work state ii					
control (N = 10) (glucose perfused)	0.78 ± 0.03	7.3 ± 0.5	48.8 ± 3.1	4.5 ± 0.2	57.1 ± 2.6
Pyr perfused (N = 10) (no glucose)	1.28 ± 0.17	4.2 ± 1.0	53.7 ± 1.5	2.3 ± 0.5	52.4 ± 3.5
Pyr perfused (N = 9) (no glucose, depleted)[b]	1.13 ± 0.12	4.3 ± 0.5	55.2 ± 3.3	2.2 ± 0.19	54.6 ± 3.0
Pyr perfused IA inhibited (N = 9)	0.85 ± 0.07	3.7 ± 0.5	50.5 ± 1.6	2.2 ± 0.28	37.6 ± 2.2

[a] Control data are reproduced from Tables I and II for work states i and ii. During pyruvate (Pyr) perfusion, pyruvate concentration was 0.5 and 1 mM for work states i and ii, respectively. [b] Depleted means depleted of endogenous carbon sources by transient perfusion with substrate-free media prior to perfusion with pyruvate.

Table V: P_i [μmol (g·dry wt)$^{-1}$] Attained during $P_i \rightarrow ATP$ Rate Measurements by Hearts Depleted of Their Endogenous Carbon Sources or Exposed to IA, and Supplied Pyruvate as the Carbon Source[a]

	i	i′	ii	iii	iv
depleted	11.9 ± 1.0		14.3 ± 1.4	13.0 ± 1.3	13.0 ± 2.0
IA inhibited	7.4 ± 0.7	11.1 ± 1.0	12.5 ± 1.6		19.2 ± 1.7

[a] All values are mean ± SEM. Both depleted and IA-inhibited hearts were supplied the same amount of pyruvate (0.5, 1, 2, and 10 mM for work states i–iv, respectively, and 0.5 mM for i′). Work state iii was not used for IA-inhibited hearts. Instead, work state i′ was employed. In this state, IA-inhibited hearts achieved MVO_2's intermediate between those attained in work states i and ii. N was 9, 10, 11, and 9 for depleted hearts at work states i–iv, respectively, and 9, 8, 9, and 7 for IA-inhibited hearts at work states i, i′, ii, and iv, respectively.

endogenous glycolytic carbon substrates. The MVO_2 and RPP values represent averages maintained by these hearts during the kinetic measurements. The expected linear relationship was evident in both cases, and this relationship was not statistically different between the IA-inhibited hearts and the others. However, the IA-inhibited hearts achieved a lower RPP and MVO_2 at work states ii and iv (Figure 6) (work state iii was not used with IA-inhibited hearts).

For direct comparison, some of the kinetic and functional measurements obtained from glucose-perfused hearts and in hearts where glycolytic activity was reduced or eliminated by the three interventions listed previously are given in Table IV for two of the four work states studied. At work state i, which achieved the lowest MVO_2 values in this study, removing glucose and supplying 0.5 mM pyruvate as the carbon source reduced the $P_i \rightarrow ATP$ rate and the $P_i \rightarrow ATP$ rate:MVO ratio significantly ($p < 0.001$) while MVO_2 remained unaltered; further reduction of the $P_i \rightarrow ATP$ rate and rate:MVO ratio was noted upon IA inhibition of GAPDH activity without a commensurate reduction of MVO_2. At work state ii, which achieved a higher MVO_2, elimination of exogenous glucose alone induced a reduction in the $P_i \rightarrow ATP$ rate and the rate:MVO ratio. Further reductions induced in these parameters by depletion of endogenous carbon sources or IA inhibition were neither very large nor satistically significant. This trend was also noted at work states that attained even higher MVO_2's, leading to the conclusion that except at the lowest MVO_2 level achieved in this study, elimination of glucose and depletion of endogenous carbon sources were sufficient to reduce the $P_i \rightarrow ATP$ rate measured by NMR to a level where IA inhibition did not induce any futher significant reductions.

T_1* changed when GAPDH/PGK activity was altered (Table IV). This is as expected. T_1* is an experimentally determined parameter that is often compared among different studies. Caution must be exercised in such comparisons since experimental conditions such as carbon substrates can clearly influence this parameter through their effect on GAPDH/PGK activity and P_i concentration.

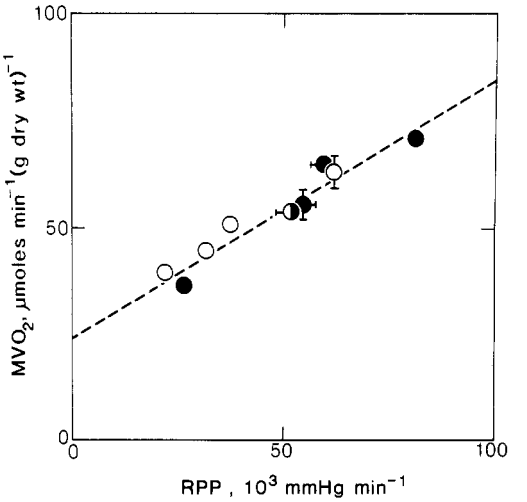

FIGURE 6: MVO_2 vs RPP relationship in pyruvate-perfused, IA-inhibited hearts (○) and hearts depleted of endogenous carbon substrates prior to perfusion with pyruvate (●). A lack of error bars indicates that the error was within the size of the symbols used. The point designated by (◑) represents a heart which was perfused with pyruvate (no glucose) but was not depleted of endogenous sources. MVO_2 and RPP shown are the average values maintained by these hearts during the kinetic measurements. The dashed line is the best fit to all data points.

The complete $P_i \rightarrow ATP$ rate data obtained on IA-inhibited hearts and on hearts where endogenous carbon sources were depleted are shown in Figure 7. The P_i levels maintained by these hearts are given in Table V. For direct comparison, the $P_i \rightarrow ATP$ rates obtained in glucose-perfused hearts (Table II) are also reproduced in Figure 7.

The $P_i \rightarrow ATP$ rates measured in the absence of the GAPDH/PGK contribution were fitted to the equation rate = K(MVO) where K is a constant; the best fit obtained by a least-squares analysis is shown as a solid line in Figure 7, with K = 2.36 ± 0.37 (SD). The rationale for this analysis is discussed in detail under Discussion. Figure 8 is a plot of

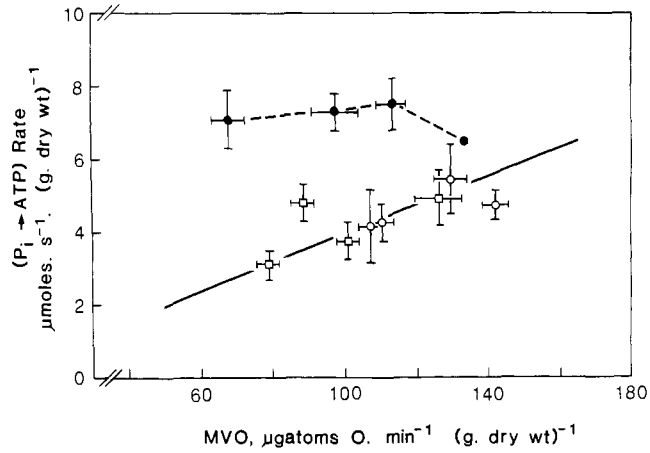

FIGURE 7: Relationship between MVO and the $P_i \rightarrow$ ATP rates measured in hearts where glucose was the primary carbon substrate (●) and in hearts where pyruvate (0.3–10 mM, depending on the work state) was supplied as the carbon source either after depletion of the endogenous carbon sources (○) or in the presence of IA inhibition of GAPDH activity (□). (●) points are reproduced from Table I. The solid line is the best fit of both (○) and (□) points to the equation rate = K(MVO).

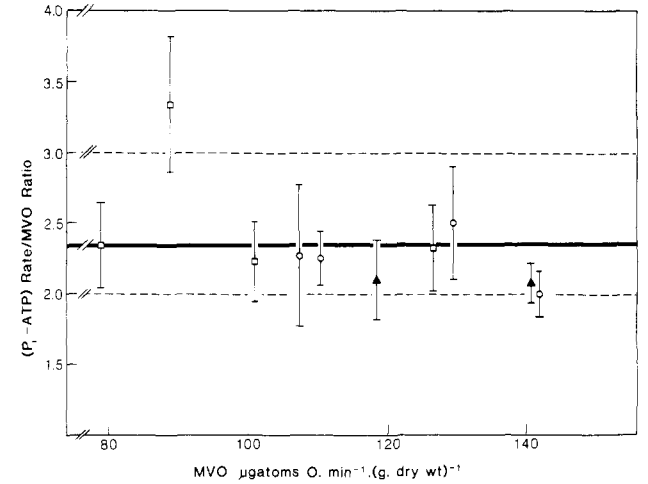

FIGURE 8: $P_i \rightarrow$ ATP rate:MVO ratio for the hearts where the GAPDH contribution was eliminated [(○) and (□) correspond to (○) and (□) points in Figure 8] and ATP → P_i rate:MVO ratio obtained from the MST measurements (▲).

the $P_i \rightarrow$ ATP rate:MVO ratio as a function of MVO. Two points obtained from ATP hydrolysis measurements (discussed later) are also included in this figure. The dashed lines correspond to the rate:MVO ratios of 2 and 3. Except for one point, the data are very tightly clustered between the values of 2.0 and 2.5. The solid line in Figure 8 shows the best fit for all data points to the equation rate/MVO = constant, obtained from *both* the $P_i \rightarrow$ ATP and ATP → P_i measurements; it corresponds to a value of 2.34 ± 0.38 (SD). $P_i \rightarrow$ ATP rate data alone obtained subsequent to elimination of the GAPDH contribution yielded a constant of 2.41 ± 0.40 (SD).

ATP → P_i Rate Measurements. In principle, it is possible to measure the ATP → P_i rate in the intact myocardium using saturation transfer. However, this measurement is rendered very difficult because the T_1 of ATPγ is inherently short and because cytosolic ATPγ exchanges rapidly with CP due to CK activity. The ATP detected in the NMR spectrum of the rat heart is virtually all cytosolic (Ugurbil et al., 1986). Therefore, when the CK contribution to the exchange is eliminated by MST, the ATP → P_i rate should contain contributions from all other reactions that utilize cytosolic ATP. These reactions include GAPDH/PGK, AK, mitochondrial translocase, and

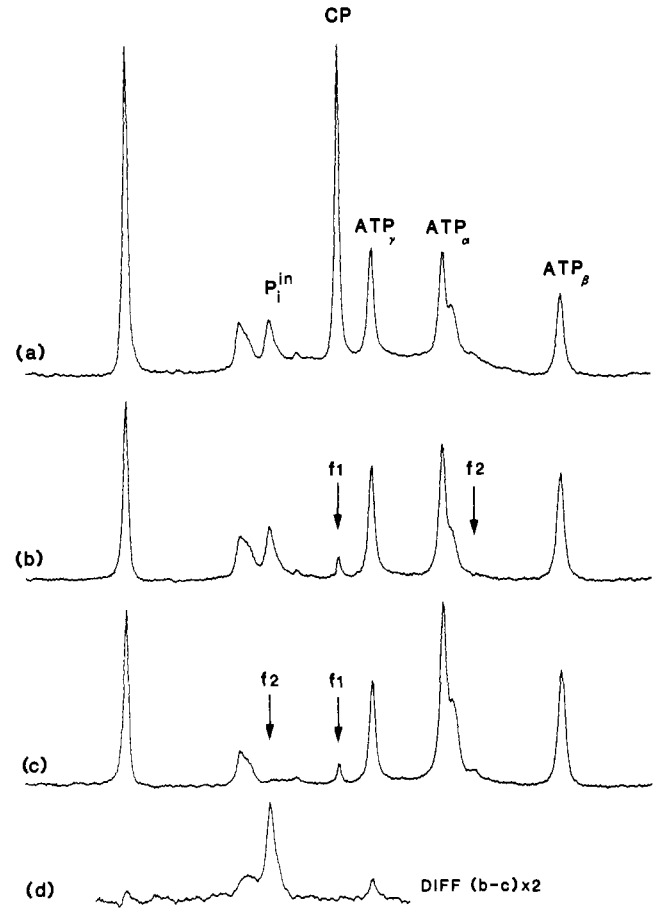

FIGURE 9: ^{31}P multiple saturation transfer (MST) spectra recorded during the measurement of the ATP → P_i rate. (a) No saturation; (b) f1 selectively saturating CP and f2 in control position; (c) f1 and f2 saturating CP and P_i peaks, respectively; (d) the difference between (c) and (b), with the vertical scale increased 2-fold for clarity. Spectrum a results from summing 28 spectra from 14 different hearts. For each spectrum, 40 FID's were collected with 90° pulses, 64-ms acquisition time, and 15-s interpulse delay. Spectra b and c result from summing 28 spectra from 14 different hearts. For each spectrum, 288 FID's were acquired in a time-averaged fashion with 90° pulses, 64-ms acquisition time, and 2.5-s interpulse delay and were processed with 30-Hz line broadening.

the various cytoplasmic ATPases. The GAPDH/PGK problem can be eliminated by procedures already outlined. We know from our studies on respiratory control that in the presence of exogenous pyruvate in amounts sufficient to fully activate pyruvate dehydrogenase, cytosolic ADP uptake into mitochondria is the rate-limiting process in oxidative phosphorylation (From et al., 1986); in this limit, translocase works primarily in the direction of ADP uptake into and ATP extrusion from the mitochondria and consequently would not contribute to the "utilization" of cytosolic ATP. The cytoplasmic ATPases such as the myosin ATPase and the (Na^+/K^+)-ATPase work predominantly if not exclusively in the ATP hydrolysis direction; this is the rate we would like to measure.

In principle, the complication introduced by the AK-mediated exchange can also be eliminated by the MST procedure. In practice, however, this is not possible since it would require continuous irradiation of the ADP_β resonance, which is not well resolved from the ATPγ peak. If the AK activity is a problem, then the rate measured by MST for ATP → P_i conversion in the cytoplasm will be underestimated.

The ATP → P_i rate measurements were performed at work states ii and iv. Figure 9 illustrates spectra from the MST measurements of the ATP → P_i rate of the highest MVO_2

Table VI: Comparison of Kinetic and Functional Data for ATP → P_i and P_i → ATP Measurements at Two Different Levels of Oxygen Consumption Rate[a]

	A		B	
	P_i → ATP	ATP → P_i	P_i → ATP	ATP → P_i
rate [μmol s^{-1} (g·dry wt)$^{-1}$]	4.3 ± 0.5	4.1 ± 0.6	4.7 ± 0.4	4.9 ± 0.4
rate:MVO ratio	2.2 ± 0.2	2.10 ± 0.28	2.0 ± 0.16	2.08 ± 0.14
MVO_2 [μmol min^{-1} (g·dry wt)$^{-1}$]	55.2 ± 3.3	59.2 ± 1.8	70.9 ± 1.7	70.3 ± 1.1
RPP (10^3 mmHg min^{-1})	54.6 ± 3.0	49.2 ± 2.8	81.2 ± 2.3	79.6 ± 2.0
N	10	11	9	14

[a] All values are mean ± SEM. P_i → ATP rate measurements were conducted in hearts depleted of their endogenous carbon substrates and supplied 1 and 10 mM pyruvate at work states ii and iv, respectively, for the lower and higher MVO_2 states. The carbon substrate was 11 mM glucose and 10 mM pyruvate for the ATP → P_i measurements, and the HR, EDP, and dobutamine exposure were those of work states ii and iv, respectively, for the lower and higher MVO_2's achieved.

achieved. These spectra were obtained by summing the spectra recorded for the different hearts at this work load. Figure 9a was recorded with no irradiation. CP was then selectively saturated in order to eliminate CP ⇄ ATP exchange (Figure 9b), and P_i was saturated by using a second selective irradiation while CK irradiation was retained (Figure 9c). A spin–lattice relaxation rate measurement was performed while both P_i and CP were saturated. The results of two MST measurements are given in Table VI. For direct comparison, P_i → ATP rates measured at comparable MVO_2's in pyruvate-perfused hearts depleted of endogenous carbon sources are also included in Table VI.

The MST measurements were performed under two different substrate conditions: (1) endogenous carbon sources were depleted, and the perfusate contained only 10 mM pyruvate (data not shown); and (2) the exogenous carbon source was 10 mM pyruvate + 11 mM glucose (Table VI). There was no significant difference in the ATP → P_i rate or the ATP → P_i rate:MVO ratio determined in the two sets of measurements. It should be noted that at work states ii and iv, the MVO_2 and RPP achieved in the presence of 10 mM pyruvate were comparable to or higher than values attained at all work states when glucose was the primary carbon source (Table II). At these high MVO_2 levels, the glycolytic contribution to the P_i → ATP rate is not very large (Figure 7). Furthermore, in the GAPDH/PGK-catalyzed ATP ⇄ P_i exchange, the ATP → P_i rate must be less than the P_i → ATP rate by twice the *net* rate of glucose consumption through glycolysis. Therefore, a difference in the ATP → P_i rates determined in the presence or absence of glucose is not expected.

Discussion

The potential for investigating the kinetics of ATP ⇄ P_i exchange using magnetization transfer measurements was realized as early as 1977 (Brown et al., 1977; Ugurbil et al., 1979). In the myocardium, there have been two early reports of P_i → ATP rate measurements using CST methods (Matthews et al., 1981; Bittl & Ingwall, 1985). As discussed previously (Kingsley-Hickman et al., 1986), both of the earlier studies suffered from erroneous assumptions about parameters required for calculating the rates. In one case, the T_1 of the

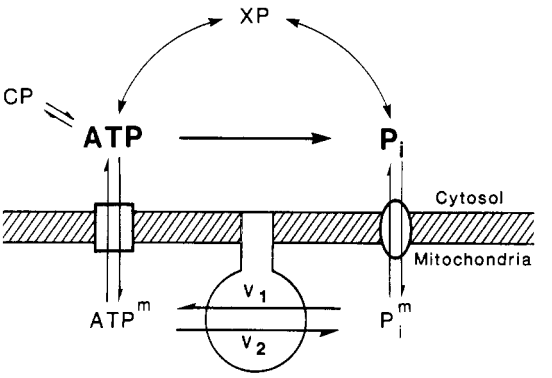

FIGURE 10: Exchange pathways between cytosolic P_i and ATP. ATP^m and P_i^m represent mitochondrial ATP and P_i, respectively.

P_i resonance in the *ischemic* myocardium was measured and assumed to be equal to the T_1 of P_i in the normoxic tissue but in the *absence* of the P_i ⇄ ATP exchange (Matthews et al., 1981). As shown by the present study, the P_i T_1 in the *absence* of the P_i ⇄ ATP exchange changes with cardiac performance. The mechanism of this alteration is not known. However, in view of this observation and the fact that the cytosolic conditions and the P_i concentration are dramatically altered during ischemia, it is not possible to justify the use of T_1 values obtained in the ischemic heart in P_i → ATP rate calculations. Even when all the parameters employed in the flux calculations are rigorously determined on each heart, it cannot be assumed that the rate measured can be used to evaluate the P:O ratio or any other kinetic property of the oxidative phosphorylation process. In fact, prior to reaching any biochemical conclusions from magnetization transfer studies of the P_i → ATP rate, three fundamental questions must be posed: (1) What is the origin of the P_i ⇄ ATP exchange monitored by NMR? (2) If contributions from all pathways other than oxidative phosphorylation are negligible or can be eliminated, is the rate determined by magnetization transfer equal to the unidirectional rate of ATP synthesis by oxidative phosphorylation? (3) If the answer to the second question is "yes", can one use the measurement to determine the P:O ratio?

The first inquiry is based on the fact that in the intact tissue, the exchange monitored by NMR between cytosolic P_i and ATP is not a simple two-site process (Figure 10). Pathways with relatively slow *net*[3] rates such as glycolysis can make significant contributions to the NMR-measurable P_i → ATP rate because magnetization transfer methods measure *unidirectional* rates; while the *net* ATP synthesis rate by a pathway can be slow, individual enzymes within this pathway can operate with rapid *unidirectional* rates.

The second question is relevant because the oxidative ATP synthesis in eukaryotic cells is compartmentalized. In the intact tissue, γ-phosphate resonances of mitochondrial and cytosolic ATP are expected to have approximately the same chemical shift. Consequently, irradiating the ATPγ resonance position will saturate both the mitochondrial and the cytosolic ATPγ spins. In this case, the rate determined by NMR is the rate of incorporation of cytosolic P_i into mitochondrial ATP. This rate is mediated by the mitochondrial P_i transport and H^+-ATPase steps. Attributing this rate to the H^+-ATPase alone requires either that the mitochondrial and cytosolic P_i pools are rapidly exchanging relative to their spin–lattice relaxation times and relative to the rate of ATP synthesis or else that the P_i transport operates unidirectionally at all times. In

[3] The *net* rate of a reaction is defined as the difference between the unidirectional rates.

the former limit, the rate measured is the *unidirectional* rate of ATP synthesis (designated as v_1 in Figure 10) by the mitochondrial H^+-ATPase. If the latter limit is applicable, then the rate of P_i extrusion from the mitochondria is negligible, and the magnetization transfer method measures only the rate of P_i transport into the mitochondria; during steady state, this rate must be equal to the *net* ATP synthesis rate by oxidative phosphorylation in the tissue. In general, mitochondrial P_i transport is thought to be rapid and not to be the rate-limiting step in mitochondrial ATP synthesis (Pederson & Wehrle, 1982). Furthermore, the density of mitochondria in the myocardium is very high. Therefore, the question pertinent to magnetization transfer studies in the heart is whether the exchange between mitochondrial and cytosolic P_i pools is sufficiently rapid to average their longitudinal relaxation. If an intermediate exchange condition prevails, the measured rate will represent a complex average of the H^+-ATPase and P_i transport kinetics.

If the potential problems due to P_i transport can be ruled out, the rate determined by CST experiments is the *unidirectional* rate of ATP synthesis by the H^+-ATPase (v_1). This rate is not necessarily related to the oxygen atom consumption rate (MVO) by the P:O ratio. If there exists a nonnegligible unidirectional rate (v_2) in the ATP $\rightarrow$ P_i direction through the H^+-ATPase, then the *net* rate of ATP synthesis ($v_1 - v_2$), and not v_1, will be proportional to MVO by the P:O ratio. This can be visualized by considering the fact that in an idealized isolated mitochondrial preparation where the transmembrane H^+ chemical potential gradient ($\Delta\mu_{H^+}$) is *not* dissipated due to leaks or energy-requiring processes, $\Delta\mu_{H^+}$ must ultimately achieve a state of equilibrium with the mitochondrial and extramitochondrial P_i, ATP, and ADP levels. At this point, in the absence of any ATP consumption and any processes that can dissipate the $\Delta\mu_{H^+}$, net ATP synthesis and O_2 consumption must cease. However, these mitochondria can still catalyze a back and forth exchange between exogenous P_i and ATP. In other words, neither v_1 nor v_2 is equal to zero but $v_1 - v_2$ is. In this domain, the ratio of v_1 (which is the rate determined by magnetization transfer) to MVO is infinity. The closest approximation to this idealized mitochondrial preparation is state 4 mitochondria which, in fact, can catalyze rapid exchange between P_i and ATPγ as shown by isotopic studies while consuming oxygen at a very slow rate (Swanson, 1956; Cohn & Drysdale, 1955; LaNoue et al., 1986).

Despite the aforementioned complexities, it is possible to establish experimentally testable criteria for evaluating the questions associated with P_i $\rightarrow$ ATP rate measurements by NMR. If the rates determined by magnetization transfer are the *net* rates of oxidative phosphorylation (i.e., $v_2 \sim 0$), then at all MVO values, they must obey the equation rate = K-(MVO) where K is a constant and is equal to the P:O ratio. A more complicated dependence on MVO would indicate that one or more of the aforementioned conditions are not fulfilled. An experimental evaluation of this condition requires simply that the P_i $\rightarrow$ ATP flux[4] is measured at different MVO's.

In glucose-perfused hearts, the P_i $\rightarrow$ ATP rate is virtually independent of MVO at the work states examined (Tables I and II). Referring to the P_i $\rightarrow$ ATP rate:MVO ratio obtained by NMR under these conditions as the P:O ratio [e.g., see Brindle and Radda (1987)] is erroneous as pointed out previously (Kingsley-Hickman et al., 1986) and discussed in greater detail in this paper. If we assume that the experimentally determined P_i $\rightarrow$ ATP rate arises exclusively from oxidative phosphorylation, then we must conclude that in glucose-perfused hearts unidirectional rates v_1 and v_2 of the H^+-ATPase are both nonvanishing and that v_1 is constant while v_2 decreases with increasing work load and MVO_2. This is the tentative conclusion that was reached in a preliminary report of this work (Kingsley-Hickman et al., 1986) and is not unreasonable in view of the fact that mitochondria can catalyze a reversible isotope exchange between extramitochondrial ATP and P_i (LaNoue et al., 1986). However, this conclusion is not supported by the data presented in Table IV and Figure 7. Instead, the data demonstrate that there exists a large glycolytic contribution to the NMR-determined rate. This is consistent with recent solution studies that have established the capability of the GAPDH/PGK enzyme couple to catalyze a P_i $\rightleftarrows$ ATP exchange measurable by saturation transfer (Brindle & Radda, 1987).

The glycolytic contribution in the myocardium (represented as the difference between the dashed and solid lines in Figure 7) is MVO_2 dependent and decreases with increasing MVO_2. At the lowest MVO_2 level, the GAPDH/PGK contribution to the unidirectional P_i $\rightarrow$ ATP rate was $\sim$4 μmol s^{-1} (g·dry wt)$^{-1}$ (Table IV). The maximum *net* rate of glucose utilization in the myocardium is $\sim$0.27 μmol s^{-1} (g·dry wt)$^{-1}$ (Kobayashi & Neely, 1979). Therefore, the reaction catalyzed by the GAPDH/PGK enzymes must be near equilibrium in glucose-perfused hearts operating at an MVO_2 of $\sim$35 μmol min^{-1} (g·dry wt)$^{-1}$; even though the reaction deviates from equilibrium with increasing MVO_2, the near-equilibrium state is maintained over a large MVO_2 range (Figure 7). These conclusions are of significance in considering the regulatory mechanisms operative in the glycolytic pathway.

Subsequent to the elimination of the GAPDH/PGK contribution, the P_i $\rightarrow$ ATP rate is satisfactorily represented by the relationship K(MVO) (Figure 7); in other words, the P_i $\rightarrow$ ATP rate:MVO ratio is a constant for all MVO values (Figure 8). In this case, the constant of proportionality, K, would be the P:O ratio. Additional checks on the validity of this conclusion are possible. If this conclusion is correct, then the P_i $\rightarrow$ ATP rates measured for oxidative phosphorylation during a steady state must equal the overall rate of ATP utilization. Under the appropriate conditions outlined under Results, the ATP utilization rate in the cytoplasm can be determined by the MST technique. Even with the MST method, however, the potential complication due to AK activity cannot be eliminated. Therefore, the ATP $\rightarrow$ P_i rate measured by MST can be equal to the P_i $\rightarrow$ ATP rate determined by CST *if and only if* AK is not a problem, and v_2 is negligible.

As illustrated in Table VI, the ATP $\rightarrow$ P_i and P_i $\rightarrow$ ATP fluxes were clearly equal within the error of the determination. Therefore, we conclude that, indeed, the H^+-ATPase is operating unidirectionally in the direction of ATP synthesis under these work load conditions (i.e., $v_2 = 0$) and AK is not a source of complication in measurements of ATP hydrolysis rates. Consequently, the fluxes obtained in both directions for the P_i $\rightleftarrows$ ATP exchange can be used to determine the P:O ratio. The P:O ratios obtained from the two MST measurements were 2.10 ± 0.28 (SEM, N = 11) and 2.08 ± 0.14 (SEM, N = 14), in excellent agreement with the value of 2.41 ± 0.40 (SD) obtained from the CST data alone in the opposite direction. As previously mentioned, the average obtained from both the CST and the MST data is 2.34 ± 0.38 (SD). Obtaining the same rates and the same P:O ratios by two different measurements gives us considerably more confidence in these numbers because the problems associated with the two dif-

[4] Following previous conventions, the terms "rate" and "flux" are used interchangeably.

ferent measurements are different.

Despite extensive studies with isolated mitochondria, the P:O ratio continues to be a controversial parameter [e.g., see recent review by Ferguson (1986)]. The suggested numbers include 2, 3, and noninteger numbers between 2 and 3 [see Ferguson (1986) and references cited therein]. In the intact tissue, the problem is more complex and the effective P:O ratio may not even be a universal constant. Because of this complexity, a distinction should be made between a "theoretical" and an "operative" P:O ratio. The former can be defined as the number of protons extruded from the mitochondria by the electron-transport chain per pair of electrons (i.e., per O atom consumed) divided by the number of protons utilized by the mitochondrial H^+-ATPase to synthesize one ATP molecule. The operative P:O ratio is the ratio that exists under the more realistic conditions where the extent of $FADH_2$ vs NADH production is not well-defined and where the electrochemical H^+ gradient across the mitochondrial membrane can be dissipated by a variety of reactions such as transport as well as by naturally occurring uncoupling agents. The P:O ratio determined in NMR studies of the intact myocardium is the operative P:O ratio. The operative P:O ratio is always less than or equal to the theoretical ratio. The operative P:O ratio may in fact be different for different tissues and may even change for a given tissue with different conditions. For example, with high concentrations of fatty acids as the exogenous carbon source, the operative P:O ratio in the myocardium may be lower than the number reported in this study.

The conclusions reached in this study can be summarized in two categories. A general conclusion is that the magnetization transfer measurements in intact tissues are extremely complicated; however, experimental criteria exist which can be used to validate the data. Such experimental evaluations must be performed for each system. More specifically, these studies have provided the following biochemically significant contributions: (1) In the MVO_2 range $\sim$30–80 μmol of O_2 min^{-1} (g·dry wt)$^{-1}$, which covers a moderate to high work load range for a rat, the mitochondrial H^+-ATPase operates *unidirectionally* in the ATP synthesis direction (i.e., it is far out of equilibrium). (2) The GAPDH/PGK-catalyzed reaction is near equilibrium in the glucose-perfused rat heart operating at moderate to low work loads. (3) In the intact myocardium, the P:O ratio determined both from MST data in the ATP $\rightarrow$ P_i direction and from the CST data in the $P_i \rightarrow$ ATP direction is significantly less than the canonically used value of 3.

Registry No. ATP, 56-65-5; P_i, 14265-44-2; CP, 67-07-2; FBP, 488-69-7; GAPDH, 9001-50-7; PGK, 9001-83-6; glucose, 50-99-7; pyruvic acid, 127-17-3.

References

Alger, J. R., & Shulman, R. G. (1984) *Q. Rev. Biophys. 17*, 83–124.

Bittl, J. A., & Ingwall, J. S. (1985) *J. Biol. Chem. 260*, 3512–3517.

Brindle, K., & Krikler, S. (1985) *Biochim. Biophys. Acta 847*, 285–292.

Brindle, K. M., & Radda, G. K. (1987) *Biochim. Biophys. Acta 928*, 45–55.

Brown, T. R., Ugurbil, K., & Shulman, R. G. (1977) *Proc. Natl. Acad. Sci. U.S.A. 74*, 5551–5553.

Campbell, S. L., Jones, K. A., & Shulman, R. G. (1985) *FEBS Lett. 193*, 189–193.

Cohn, M., & Drysdale, G. R. (1955) *J. Biol. Chem. 216*, 831–846.

Dennis, S. C., Padma, A., DeBuysere, M. S., & Olson, M. S. (1979) *J. Biol. Chem. 254*, 1252–1258.

Ferguson, S. J. (1986) *Trends Biochem. Sci. (Pers. Ed.) 11*, 351–353.

From, A. H. L., Petein, M. A., Michurski, S. P., Zimmer, S. D. & Ugurbil, K. (1986) *FEBS Lett. 206*, 257–261.

Hutter, J. F., Schweickhardt, C., Piper, H. M., & Spieckermann, P. G. (1984) *J. Mol. Cell. Cardiol. 16*, 105–108.

Kingsley-Hickman, P., Sako, E. Y., Andreone, P. A., St. Cyr, J. A., Michurski, S., Foker, J. E., From, A. H. L., Petein, M., & Ugurbil, K. (1986) *FEBS Lett. 198*, 159–163.

Kobayashi, K., & Neely, J. R. (1979) *Circ. Res. 44*, 166–175.

Koretsky, A. P., & Weiner, M. W. (1984) in *Biomedical Magnetic Resonance* (James, T. L., & Margulis, A. R., Eds.) pp 209–230, Radiology Research and Education Foundation, San Francisco.

La Noue, K. F., Jeffries, F. M. H., & Radda, G. K. (1986) *Biochemistry 25*, 7667–7675.

Matthews, P. M., Bland, J. L., Gadian, D. G., & Radda, G. K. (1981) *Biochem. Biophys. Res. Commun. 103*, 1052–1059.

Nageswara Rao, B. D., Cohn, M., & Scopes, R. K. (1978) *J. Biol. Chem. 253*, 8056–8060.

Nageswara Rao, B. D., Cohn, M., & Scopes, R. K. (1979) *J. Biol. Chem. 254*, 4933.

Pedersen, P. L., & Wehrle, J. P. (1983) *Membr. Transp. 1*, 645–663.

Swanson, M. A. (1956) *Biochim. Biophys. Acta 20*, 85–91.

Thoma, W. J., & Ugurbil, K. (1987) *Biochim. Biophys. Acta 893*, 225–231.

Ugurbil, K. (1985a) *Circulation 72 (Suppl. 4)*, 94–96.

Ugurbil, K. (1985b) *J. Magn. Reson. 64*, 207–219.

Ugurbil, K., Petein, M., Maidan, R., Michurski, S., & From, A. H. L. (1986) *Biochemistry 25*, 100–107.